# Effect of Pulse Temporal Profile on Autler–Townes Splitting in Photoelectron Spectrum *

YUAN Kai-Jun(元凯军), SHU Chuan-Cun(束传存), CONG Shu-Lin(丛书林)**
*Department of Physics, Dalian University of Technology, Dalian 116024*

(Received 10 July 2006)

*The effect of pulse temporal profiles on the Autler–Townes (AT) splitting in photoelectron spectra is theoretically studied by employing the time-dependent wave packet method for a rotational $Na_2$ molecule. The AT splitting which results from the sufficient Rabi oscillations is affected by the pulse profile and molecular alignment. The AT splitting may be observed only by utilizing proper pulse profiles with a certain intensity.*

*PACS: 33. 80. Eh, 42. 50. Hz, 82. 53. Kp*

With the development of ultrashort laser pulses, many new phenomena have been investigated and discovered in the femtosecond time region.[1−11] Exposing the atomic and molecular systems to ultrashort laser pulse fields, some fascinating, even unexpected, phenomena have been observed. Owing to the ultrashort duration, the driven pulses allow the direct observation of chemical reactions on the time scale in which they occur. This has led to tremendous progress in understanding chemical and biological processes. The relevant laser parameters, such as the intensity, width and the shape of the pulse, have been used to manipulate the molecular reaction dynamics.

Autler–Townes (AT) splittings of atoms and molecules have been observed and investigated.[12−16] Using one-dimensional wave packet dynamics simulations, Sun and Lou[16] observed the AT splitting in the photoelectron spectrum of $Na_2$ molecules. However, the effect of the molecular alignment should be considered in the practical dynamics studies.[17−19] The AT splitting comes from the rovibrational coherent states belonging to different electronic potential energy curves in the molecular multiphoton resonance ionization spectrum. It results from efficient Rabi oscillations within the resonant region during the laser-molecule interaction. Due to the effects of the molecular rotation and alignment, the Rabi oscillations will dampen, which causes the AT splitting to weaken, even to vanish. However, when we choose a proper pulse temporal profile, the evident AT splitting can be observed for the rotational molecule that undergoes a well alignment. In this Letter, the time-dependent wave packet method is used to numerically simulate the AT splitting in the photoelectronic spectrum of the $Na_2$ molecule.

The three electronic states of the $Na_2$ molecule,[20] the ground state $1^1\Sigma_g^+$, the double minimum state $2^1\Sigma_u^+$, and the ionic ground state $1^2\Sigma_g^+$, are employed to simulate the dynamics of the AT splitting. For convenience, the electronic states $1^1\Sigma_g^+$, $2^1\Sigma_u^+$ and $1^2\Sigma_g^+$ are abbreviated to $|X\rangle$, $|S\rangle$ and $|I\rangle$, respectively. In the present work the linearly polarized laser fields are used and only the $\Delta M = 0$ transitions are considered. The $Na_2$ molecule is described by the azimuthally symmetric Hamiltonian. In the Born–Oppenheimer frame, the wavefunctions $\psi(R,\theta,t)$ of the three electronic states are obtained by solving the time-dependent Schrödinger equation (TDSE) with Hamiltonian:[21]

$$\hat{H}(R,\theta,t) = \hat{H}_0(R,\theta) + \hat{H}_{\rm I}(R,\theta,t), \tag{1}$$

with molecular Hamiltonian

$$\begin{aligned}\hat{H}_0(R,\theta) &= \hat{T}_R + \hat{T}_\theta + \hat{V}(R) \\ &= -\frac{\hbar^2}{2m}\frac{\partial^2}{\partial R^2} - \frac{\hbar^2}{2mR^2}\frac{1}{\sin\theta}\frac{\partial}{\partial\theta}\Big(\sin\theta\frac{\partial}{\partial\theta}\Big) \\ &\quad + \hat{V}(R),\end{aligned} \tag{2}$$

where $m$ is the reduced mass of the molecule, $R$ the internuclear separation, and $\theta$ the angle between the molecular axis and the laser electric field (space fixed) axis. $\hat{V}(R)$ represents the potential curves of the three electronic states. The interaction Hamiltonian can be expressed as

$$\hat{H}_{\rm I}(R,\theta,t) = -\mu(R)\cos\theta\varepsilon(t). \tag{3}$$

The laser field is given by

$$\varepsilon(t) = \varepsilon_0 f(t)\cos(\omega t), \tag{4}$$

where $\varepsilon_0$ is the peak intensity; $\omega$ is the photon energy of the laser pulse; $f(t)$ denotes the pulse temporal profile; $\mu(R)$ is the transition dipole moment between the electronic states.

The ionization continuum can be discretized into a band of quasicontinuum levels in terms of the electron eigenstates $E$ containing the core and free electron.[17,22−25] The states are labelled according to the kinetic energy of the ejected electron:

$$|\chi(R,\theta,t)\rangle = \sum_{n=1}^{N}\psi(R,\theta;E_n,t)|E_n\rangle, \tag{5}$$

* Supported by the National Natural Science Foundation of China under Grant No 10374012.
** To whom correspondence should be addressed. Email: shlcong@dlut.edu.cn
©2006 Chinese Physical Society and IOP Publishing Ltd

where $E_1$ and $E_N$ are the smallest and largest energies which can be transferred to the electron, respectively; $\psi(R,\theta;E_n,t)$ are the wavefunctions of $Na_2^+$, corresponding to the emission of an electron with kinetic energy $E_n$. This leads to a Hamiltonian matrix of dimensions $(N+2)(N+2)$, including two neutral states and $N$ ionization quasicontinuum states; $N$ is chosen to be 40 in this work.

We use the Fourier grid Hamiltonian (FGH) method[26] to obtain the radial eigenfunctions and Legendre polynomials as the eigenfunctions for the angular variable $\theta$. When the Legendre polynomials $P_l(\cos)$ are chosen as angular basis sets, the Gauss–Legendre quadrature points are used as the grid points. The points can be easily found by the discrete variable representation (DVR) technique.

The propagation of the wavefunction $\psi(R,\theta,t)$ is accomplished by the split operator method.[27] $\hat{T}_R$ is transformed between momentum and coordinates space using the fast Fourier transform (FFT) technique[28] and $\hat{T}_\theta$ is switched forwards and backwards between the coordinate representation and the polynomial representation by the DVR technique.[29] For each of them the representation transform is found while the other variables are fixed. The coupled matrix $\hat{V}(R)+\hat{H}_{\rm I}(R,\theta,t)$, diagonalized in coordinate space, acts on the wavefunction directly in the coordinate space by multiplication.[30–32]

The time-dependent population in the electronic state $|S\rangle$ is obtained from the numerical calculation

$$P(t)=\int \sin\theta d\theta \int |\psi(R,\theta,t)|^2 dR, \qquad (6)$$

and the photoelectron spectrum is defined as

$$P_{\rm I}(E_n)=\lim_{t\to\infty}\int \sin\theta d\theta \int |\psi(R,\theta;E_n,t)|^2 dR. \qquad (7)$$

The expectation value of $\langle\cos^2\theta\rangle$, which characterizes the molecular alignment, can be expressed as

$$\langle\cos^2\theta\rangle(t)=\frac{\int \sin\theta\cos^2\theta d\theta \int |\psi(R,\theta,t)|^2 dR}{\int \sin\theta d\theta \int |\psi(R,\theta,t)|^2 dR}. \qquad (8)$$

This quantity ranges from 1.0 for an idealized perfectly aligned sample along the laser polarization axis, to 0 where the molecular axis is perpendicular to the polarization axis (antialignment).

In the dynamics simulations, the Condon approximation is used. The transition dipole moment $\mu_{XS}$ given by Konowalow *et al.*[33] is employed and $\mu_{\rm SI}$ is taken as $\mu_{\rm SI}=\mu_{XS}/20$.[20] The center wavelength of the laser pulse is 340 nm.

We only consider the case of the initial wavefunction to be the ground vibrational state of the electron $|X\rangle$ state with rotational quantum number $J_0=0$. We first investigate the excitation and ionization of the $Na_2$ molecule in a rectangle-like laser pulse. The peak intensity of the pulse is $2.5\times10^{11}\,{\rm W/cm^2}$ and the pulse temporal profile (pulse I) is given by

$$f(t)=\begin{cases}\sin\dfrac{\pi(t-t_1)}{\tau}, & t\le t_1,\\ 1, & t_1\le t\le t_2,\\ \sin\dfrac{\pi(t_2-t)}{\tau}, & t\ge t_2,\end{cases} \qquad (9)$$

where $t_1=t_0-(T+\tau)/2$; $t_2=t_0+(T+\tau)/2$; and $t_0$ denotes the center time of pulse. The temporal parameter $\tau$ and plateau duration $T$ are taken to be 10 fs and 25 fs, respectively. Figure 2 depicts the photoelectron spectrum and the time evolution of the population $P(t)$ in the $|S\rangle$ state of the $Na_2$ molecule. It can be seen that the photoelectron spectrum consists of two separate peaks at about 2.17 and 2.43 eV. The manifest Rabi oscillations appear in the population $P(t)$.

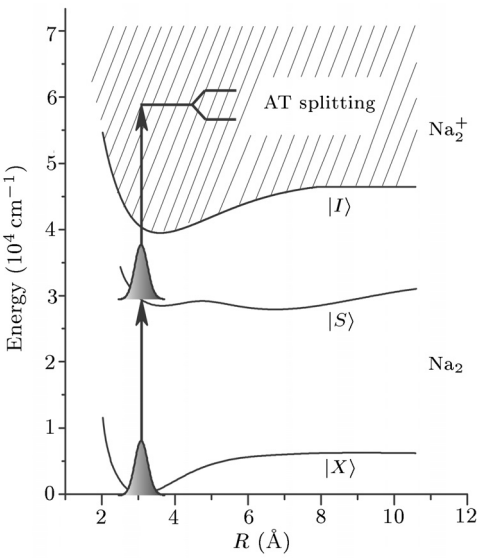


**Fig. 1.** The potential energy curves of the electronic states involved the two-photo resonance photoionization of the $Na_2$ molecule.

For the $Na_2$ molecule, the rotational and vibrational periods are much longer than the duration of the driven pulse. Therefore, the coherent rovibrational wave packet can be created in the $|S\rangle$ electronic state by the ultrashort pulse. When Rabi oscillations are sufficiently strong, the doublet structure will appear in the photoelectron spectrum. This pattern of the photoelectron spectrum splitting can be regarded as the AT splitting which comes from two strongly coupled coherent rovibrational states evolving along their own molecular potential curves, i.e. the AT splitting is induced by the sufficient Rabi oscillations shown in Fig. 2(b).

However, the molecular dynamics change drastically when we use a laser pulse with the sinusoid temporal profile (pulse II):

$$f(t)=\begin{cases}\sin\left(\dfrac{\pi t}{\tau_0}\right), & t_0-\dfrac{\tau_0}{2}\le t\le t_0+\dfrac{\tau_0}{2},\\ 0, & \text{otherwise},\end{cases} \qquad (10)$$

where $t_0$ and $\tau_0(= 35\,\text{fs})$ are the center time and the duration time of pulse. The peak intensity $\varepsilon_0$ of the laser pulse is also $2.5 \times 10^{11}\,\text{W/cm}^2$. Figure 3 shows the photoelectron spectrum and population distribution $P(t)$ of the $|S\rangle$ state. The photoelectron spectrum only exhibits a smooth peak at about 2.30 eV. The Rabi oscillations are not manifest as that with pulse I. In this case, the AT splitting in the photoelectron spectrum cannot be observed without the efficient Rabi oscillations.

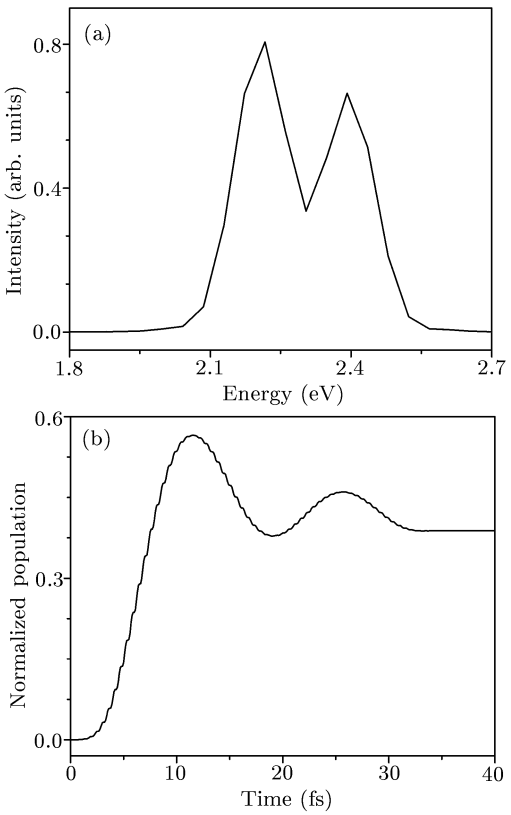


**Fig. 2.** (a) The photoelectron spectrum simulated by using the quantum wave packet method. (b) The population $P(t)$ in the $|S\rangle$ state. The rectangle-like laser pulse I with intensity $\varepsilon_0 = 2.5 \times 10^{11}\,\text{W/cm}^2$ is used.

The dynamics of the AT splitting with the pulse Ⅱ is less robust than that with the pulse I. This is reflected in the sensitivity of the dynamics with respective to the pulse temporal profiles. When coherent radiation is resonant, the excitation probability $P(t)$ follows the area theorem

$$P(t) \propto \sin^2 \sigma(t), \tag{11}$$

where $\sigma(t)$ is the pulse area

$$\sigma(t) = \int_{-\infty}^{t} \Omega(t')dt', \tag{12}$$

with Rabi frequency $\Omega(t)$ being a function of the laser power characterized by the angular variable $\theta$. The expectation value of $\cos^2\theta$ describes the alignment of the molecular axis in the space fixed frame. The time evolutions of the expectation values of $\cos^2\theta$ in the

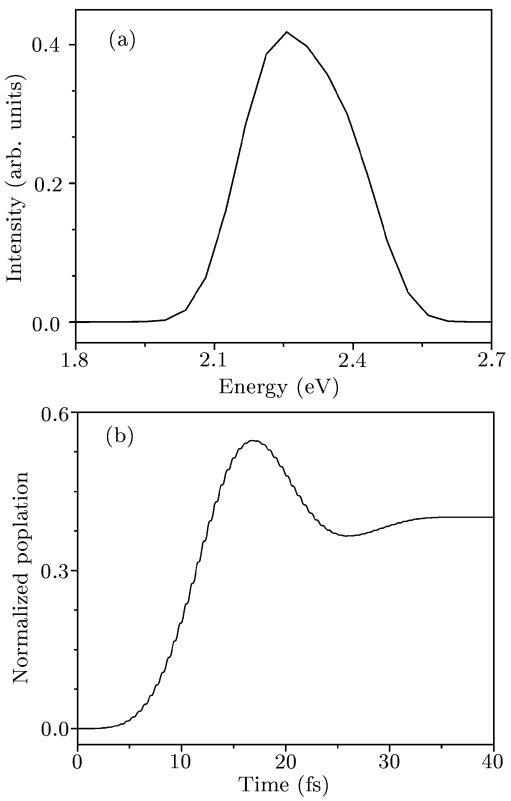


**Fig. 3.** (a) The photoelectron spectrum simulated by using the quantum wave packet method. (b) The population $P(t)$ in the $|S\rangle$ state. The sinusoid laser pulse Ⅱ with intensity $\varepsilon_0 = 2.5 \times 10^{11}\,\text{W/cm}^2$ is used.

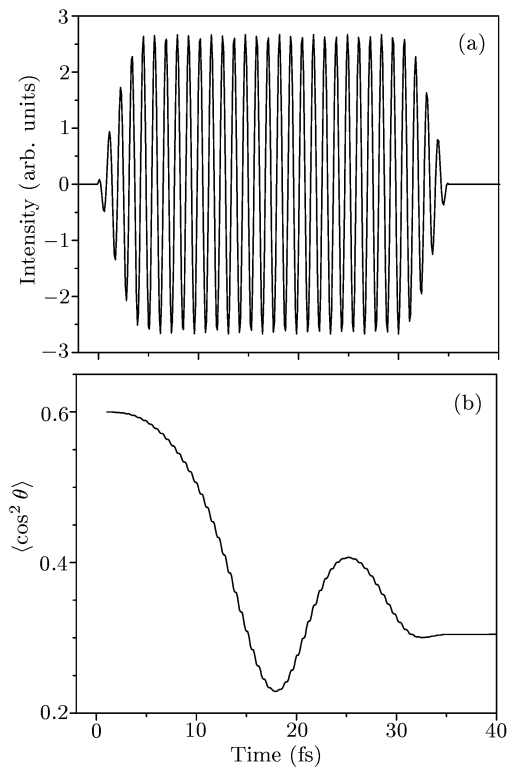


**Fig. 4.** (a) The laser pulse I with the intensity $\varepsilon_0 = 2.5 \times 10^{11}\text{W/cm}^2$. (b) Time evolution of $\langle\cos^2\theta\rangle$ in the $|S\rangle$ state.

$|S\rangle$ state with pulses I and II, including the pulse profiles, are depicted in Figs. 4 and 5. Initially, the maximal alignment $\langle\cos^2\theta\rangle$ in the $|S\rangle$ electronic state is 0.6, corresponding to randomly aligned molecules. Then the value of alignment parameter $\langle\cos^2\theta\rangle$ decreases with the increase of time, meaning that the molecular axis trends toward the direction perpendicular to the laser field. With pulse I, the alignment parameter $\langle\cos^2\theta\rangle$ can reach 0.41 at $t \approx 26$ fs. In this case, the pulse area is enough to cause the well defined Rabi oscillations, and the AT splitting can be observed. However, with pulse II, the alignment parameter $\langle\cos^2\theta\rangle$ decreases drastically. For the second 'peak' of the population in the $|S\rangle$ state, $\langle\cos^2\theta\rangle < 0.37$. As a result, the AT splitting (separate peaks) in the photoelectron spectrum cannot be observed in Fig. 3(a).

Moreover, with a longer pulse, the motion of the wave packet in the excited $|S\rangle$ state can not be ignored anymore. The excited wave packet moves away from the resonance region during the laser–molecule interaction. The Rabi oscillations are less pronounced. Thus the AT splitting could be hardly observed.[16]

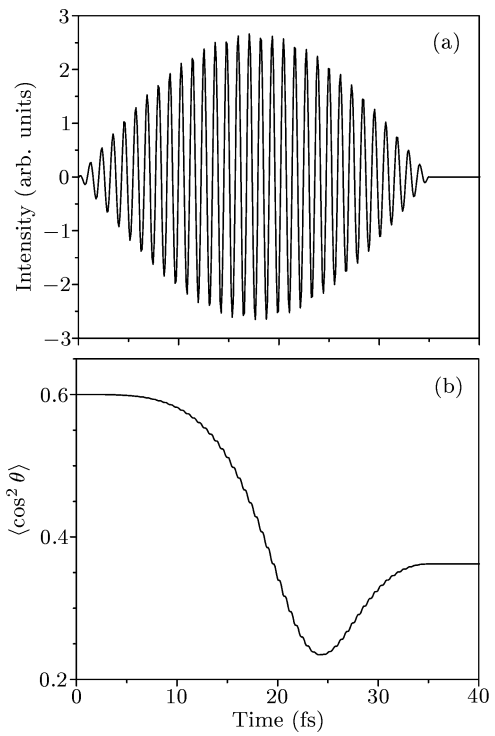


**Fig. 5.** (a) The laser pulse II with the intensity $\varepsilon_0 = 2.5 \times 10^{11}$ W/cm$^2$. (b) Time evolution of $\langle cos^2\theta\rangle$ in the $|S\rangle$ state.

In summary, the effect of the pulse temporal profile on the AT splitting is theoretically investigated using the time-dependent quantum wave packet method for the $Na_2$ molecule in femtosecond laser field. The AT splitting comes from the efficient Rabi oscillations within the resonant region during the laser-molecule interaction. Altering the pulse temporal profile can change the degree of the molecular alignment. The rectangle-like envelope laser pulse with shorter switch-on and -off time produces the well defined Rabi oscillations during the exciting process. Thus the distinct AT splitting is observed. However, for the sinusoid pulse with longer leading and tailing edges, the adequate Rabi oscillations that induce the AT splitting cannot be acquired in the photoelectron spectrum.

# References


[1] Zewail A H 2000 *J. Phys. Chem.* A **104** 5660
[2] Wang B B , Chen J, Liu J, Li X F and Fu P M 2005 *Chin. Phys. Lett.* **22** 2237
[3] Cen Y, Ma J, Zhu R Y, Lu J J, Qian S X and Chen J Y 2004 *Chin. Phys. Lett.* **21** 1636
[4] Bai L H, Zhang J T and Xu Z Z 2005 *Chin. Phys. Lett.* **22** 853
[5] Zhang X Y, Sun Z R, Chen G L, Wang Z G, Xu Z Z and Li R X 2004 *Chin. Phys. Lett.* **21** 1930
[6] Zhang H, Han K L, Zhao Y, He G Z and Lou N Q 1997 *Chem. Phys. Lett.* **271** 204
[7] Zhang H, Han K L, He G Z and Lou N Q 1998 *Chem. Phys. Lett.* **289** 494
[8] Hu J, Han K L, He G Z 2005 *Phys. Rev. Lett.* **95** 123001
[9] Wollenhaupt M, Engel V and Baumert T, 2005 *Ann. Rev. Phys. Chem.* **56** 25
[10] GeBer O, Lee A M D, Shaffer J P, Reisler H, Levchenko S V, Krylov A I, Underwood J G, Shi H, East A L L, Wardlaw D M, Chrysostom E T H, Hayden C C and Stolow A 2006 *Science* **311** 219
[11] Sun Z G, Liu H P, Lou N Q and Cong S L 2003 *Chem. Phys. Lett.* **369** 374
[12] Autler S H and Townes C H 1955 *Phys. Rev.* **100** 703
[13] Xu S, Sha G, Jiang B, Sun W, Chen X and Zhang C 1994 *J. Chem. Phys.* **100** 6122
[14] Qi J, Lazarov G, Wang X, Li L, Narducci L M, Lyyra A M and Spano F C 1999 *Phys. Rev. Lett.* **83** 288
[15] Zhao Y T, Zhao J M , Huang T, Xiao L T and Jia S T 2005 *Chin. Phys. Lett.* **22** 1668
[16] Sun Z G and Lou N Q 2003 *Phys. Rev. Lett.* **91** 023002
[17] Friedrich B and Herschbach D 1995 *Phys. Rev. Lett.* **74** 4623
[18] Granucci G, Magnier S and Persico M 2002 *J. Chem. Phys.* **116** 1022
[19] Stapelfeldt H and Seideman T 2003 *Rev. Mod. Phys.* **75** 543
[20] Meier C and Engel V 1994 *J. Chem. Phys.* **101** 2673
[21] Andrianov I V and Paramonov G K 1999 *Phys. Rev.* A **59** 2134
[22] Wang S M, Cong S L, Yuan K J and Yu J 2005 *Chem. Phys. Lett.* **401** 509
[23] Wang S M, Cong S L, Yuan K J and Niu Y Y 2005 *Chem. Phys. Lett.* **417** 164
[24] Wang S M, Yuan K J and Cong S L2006 *Chin. Phys. Lett.* **23** 87
[25] Yuan K J, Wang S M and Cong S L 2005 *Chin. Phys. Lett.* **22** 2534
[26] Marston C C and Balint-Kurti G G 1989 *J. Chem. Phys.* **91** 3571
[27] Feit M D and Fleck J A 1983 *J. Chem. Phys.* **78** 301
[28] Kosloff D and Kosloff R 1983 *J. Comput. Phys.* **35** 52
[29] Yuan K J, Sun Z, Wang S M and Cong S L 2005 *Chem. Phys. Lett.* **414** 180
[30] Sun Z G, Cong S L, Lou N Q and Han K L 2002 *Chem. Phys. Chem.* **3** 976
[31] Yuan K J, Sun Z G, Cong S L, Wang S M, Yu J and Lou N Q 2005 *Chem. Phys.* **316** 245
[32] Yuan K J, Sun Z, Cong S L and Lou N 2005 *Phys. Rev.* A **72** 052513
[33] Konowalow D D, Rosenkrantz M E and Hochhauser D S 1983 *J. Mol. Spectrosc.* **99** 321